Astronomische Nachrichten

Astronomische Nachrichten

PROCEEDING

Particle Acceleration in Solar Flares From Radio and Hard X-Ray Spectra

Adriana Valio[1] | Douglas F. daSilva[1,2] | Hui Li[2]

[1]Centro de Rádio Astronomia e Astrofísica Mackenzie, Universidade Presbiteriana Mackenzie, São Paulo, Brazil | [2]State Key Laboratory for Space Weather, National Space Science Center, Chinese Academy of Sciences, Beijing, China

Correspondence: Adriana Valio (avalio@craam.mackenzie.br)

Received: 4 December 2024 | **Accepted:** 5 December 2024

Funding: This work was supported by the Brazilian agency FAPESP (grants #2018/04055-8 and #2021/02120-0), the China-Brazil Joint Laboratory for Space Weather (CBJLSW), the International Partnership Program of Chinese Academy of Sciences (Grants 183311KYSB20200003 and 183311KYSB20200017), and NNSFC grants (42374198 and 42188101).

Keywords: particle acceleration | radio emission | solar flares

ABSTRACT

For a deeper understanding of the physical processes at play in solar flares, it is necessary to analyze the flare emissions at multiple wavelengths. This multifrequency approach enables the characterization of energetic electrons accelerated from hundreds of keV and up to several tens of MeV. This study reports on the observation of 10 solar flares, in which the spectral parameters were determined for the cm/mm and x-ray bands. The radio spectrum was fitted using gyrosynchrotron emission whereas the hard x-rays fit considered a model of thermal plus nonthermal emission of accelerated electrons. The results show that the spectral indices of the energy distribution of nonthermal electrons emitting in millimeter and hard x-rays do not agree, with the millimeter spectral index being approximately 2 units harder than that of hard x-rays. These findings are consistent with previous research and suggest the existence of a break in the energy spectrum of accelerated electrons. Moreover, for the only flare where photons exceeding 1 MeV were detected, the hard x-ray spectra exhibited a broken power-law where the index of the electron distribution above ∼500 keV agreed with the inferred radio spectral index.

1 | Introduction

Solar flares are among the most energetic phenomena in the Solar System, capable of releasing up to 10^{32} ergs of energy in a single event. These flares are characterized by a sudden release of energy that occurs over just a few seconds to minutes, producing intense bursts of radiation across the electromagnetic spectrum, from radio waves to x-rays and gamma rays. The primary source of this immense energy is the Sun's magnetic field, which, when twisted and stressed by plasma flows, can reconnect and rapidly release stored magnetic energy.

The released magnetic energy goes into accelerating particles to quasi-relativistic energies. These particles then travel from the magnetic reconnection site, believed to be located above the loop tops, downwards to the footpoints. Some energetic particles become trapped within the loops, and as they spiral along the magnetic field lines, they emit gyrosynchrotron radiation at radio wavelengths. As the pitch angle changes, these particles escape from the magnetic trap and collide with the chromosphere below. When they are slowed down by Coulomb forces during interactions with the positive nuclei of the ambient plasma, hard x-rays are generated through nonthermal bremsstrahlung.

As particles collide and interact within this turbulent environment, they heat the surrounding plasma to millions of degrees, causing it to emit intense x-rays and ultraviolet radiation. This localized heating and particle acceleration not only shape the solar atmosphere but also impact space weather, as these particles and radiation can disrupt satellite communications, navigation systems, and even pose risks to astronauts in space.

2 | Solar Flares

The Shibata and Magara (2011) flare model is a widely accepted model for explaining how solar flares release energy, accelerate particles, and produce various forms of radiation. In this model, the primary driver of flare energy release is magnetic reconnection, which occurs in the Sun's atmosphere when oppositely directed magnetic field lines break and reconnect. This process releases vast amounts of stored magnetic energy, accelerating particles to high energies.

Magnetic reconnection in the corona creates electric fields that accelerate electrons and ions to extremely high velocities, producing nonthermal, high-energy particles. These accelerated particles travel along magnetic field lines, some moving downward toward the dense layers of the solar atmosphere, like the chromosphere, whereas others escape along open magnetic field structures into interplanetary space.

These accelerated particles produce radiation through two main processes: gyrosynchrotron radiation and nonthermal bremsstrahlung. As the high-energy electrons spiral along the magnetic field lines in the looptops, they emit gyrosynchrotron radiation. This type of radiation is produced mainly at radio and microwave wavelengths. The intensity and spectrum of gyrosynchrotron radiation provide insights into the magnetic field strength and particle energy distribution in the flaring region.

When the accelerated electrons travel downward and collide with the dense plasma in the chromosphere, they undergo nonthermal bremsstrahlung, emitting hard x-rays as they decelerate in the presence of atomic nuclei. Nonthermal bremsstrahlung serves as a key observational signature of particle acceleration during flares, as it reflects the interaction of nonthermal electrons with the chromospheric plasma.

The energy released by magnetic reconnection also heats the surrounding plasma to tens of millions of degrees, creating hot, dense loops in the corona. This heated plasma emits thermal x-rays and extreme ultraviolet (EUV) radiation, adding to the flare's radiative output.

The Shibata and Magara (2011) model thus provides a comprehensive framework for understanding how solar flares produce intense, multi-wavelength radiation by converting magnetic energy into particle acceleration, which emit radio waves by gyrosynchrotron, and hard x-rays (HXR) by nonthermal bremsstrahlung emissions. This model helps explain the complex observational features of flares and the dynamics of energy release in solar magnetic fields.

2.1 | Electron Energy Spectrum

The energy distribution of the accelerated electrons is often described as a power law such as the one depicted in the upper panel of Figure 1. According to (Tandberg-Hanssen and Emslie 2009), the accelerated electron spectra is given by:

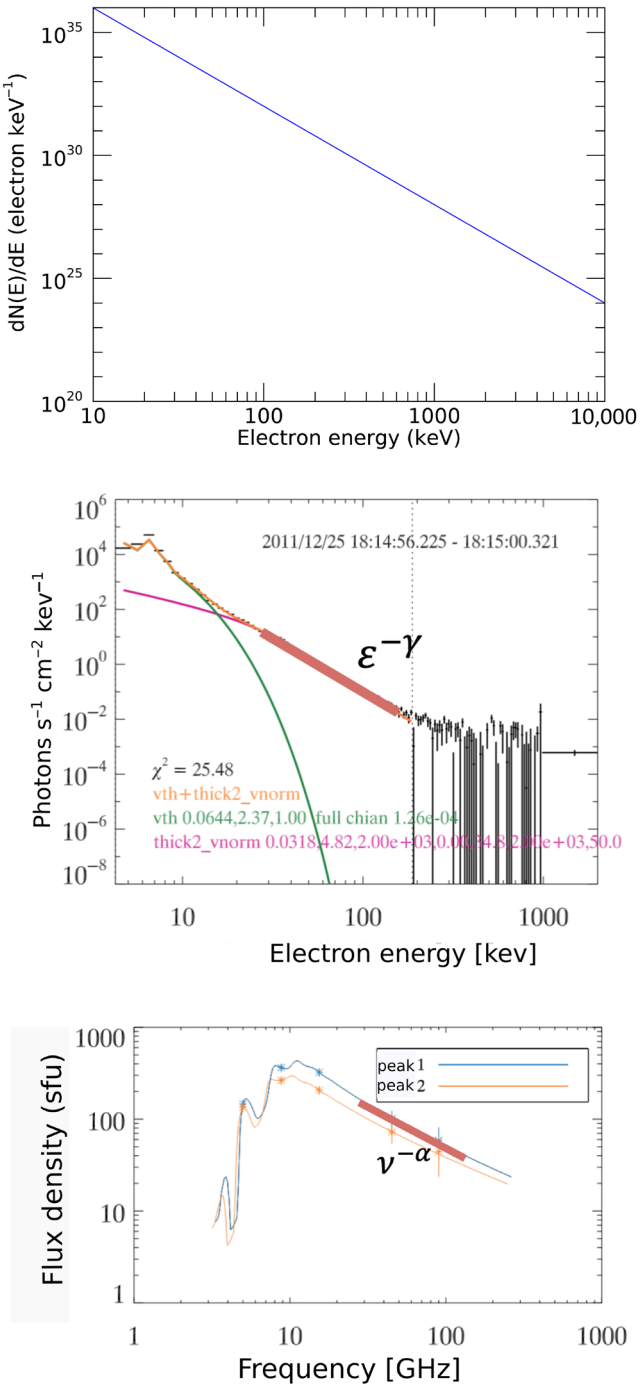

FIGURE 1 | Top: Schematics of a power-law energy spectrum of accelerated electrons. Middle: Observed photon spectra of the flare on December 25, 2011 with the power-law portion of the spectra shown by the brown line. Bottom: Radio spectra of the same flare at two time intervals (see Figure 3) the optically thin power-law emphasized by the brown line.

$$\frac{dN}{dE} = KE^{-\delta} \tag{1}$$

where K is a normalization constant. Considering that the total number of electrons, is N_{total}, with energy between a minimum, E_{min}, and a maximum energy, E_{max}:

$$N_{\text{total}} = \int_{E_{\text{min}}}^{E_{\text{max}}} KE^{-\delta}\, dE \tag{2}$$

the normalization constant is:

$$K = N_{\text{total}} \frac{\delta - 1}{E_{\text{min}}^{1-\delta} - E_{\text{max}}^{1-\delta}} \tag{3}$$

In the case of a power-law energy distribution of the electrons, the nonthermal bremsstrahlung spectra will also be a power-law (see middle panel of Figure 1). Moreover, the spectral index, δ_X, of the electron energy distribution will determine the (HXR) photon spectra, γ (Tandberg-Hanssen and Emslie 2009):

$$\delta_X \approx \gamma + 1.5 \quad \text{for } E < 100\,\text{keV} \tag{4}$$

$$\delta_X \approx \gamma + 1 \quad \text{for } E \geq 100\,\text{keV} \tag{5}$$

The radio spectrum produced by gyrosynchrotron radiation of this same population of accelerated electrons will also be a power-law in the optically thin regime (see bottom panel of Figure 1), with the radio spectral index, α, related to the electron energy distribution δ_r, given by (Dulk 1985):

$$\delta_r = 1.11\alpha + 1.36 \tag{6}$$

Here, we analyze 10 solar flares during the years of 2012 and 2013, which were observed in x-rays and radio wavelengths. We used x-ray observations from RHESSI (Lin et al. 2004) and radio observations from POEMAS (at 45 and 90 GHz, Valio et al. (2013)) and RSTN (from 1 to 15 GHz) for each event. From the multi-wavelength data, we constructed the HXR and radio spectra and measured the spectral indices: γ from the x-rays and α from the radio observations.

3 | Observation

The RHESSI satellite, a HXR telescope led by Principal Investigator Bob Lin, operated from 2002 to 2018 (Lin and Rhessi Team 2002), and is shown in the left panel of Figure 2. The HXR telescope was designed to observe solar flares, capturing images and spectra in the energy range of 3 keV to 20 MeV. RHESSI provided valuable data on the high-energy processes in solar flares, contributing significantly to our understanding of solar physics.

The POEMAS (POlarized Emission of Millimetric Activity from the Sun) radio telescope has been operating at CASLEO in Argentina, at 2550 m altitude, since November 2011 (Valio et al. 2013), and is shown in the right panel of Figure 2. It observes the Sun at two frequencies, 45 and 90 GHz, and is capable of measuring circular polarization. With a high temporal resolution of 10 ms, POEMAS provides continuous monitoring of solar activity, enabling detailed studies of rapid solar phenomena.

The RSTN (Radio Solar Telescope Network) observes the Sun at multiple microwave wavelengths (Guidice et al. 1981). Here, we used only the highest frequencies of 2.7, 5.0, 8.8, and 15.4 GHz. With four stations distributed across different longitudes, the RSTN can provide nearly uninterrupted data on solar activity, ensuring that solar radio emissions are continuously observed throughout the day. This global setup is essential for real-time monitoring and analysis of solar flares. The four RSTN stations are located at San Vito dei Normanni Air Station (Italy), Learmonth Solar Observatory (Australia), Sagamore Hill Observatory (Massachusetts, USA), and Palehua Solar Observatory (Hawaii, USA).

Observations in x-rays from RHESSI and in radio frequencies from POEMAS (45 and 90 GHz) and RSTN (1–15 GHz) provide crucial data for analyzing solar flares and energetic events in the solar atmosphere. The 10 solar flares analyzed here are listed in Table 1.

The light curves of the flare that occurred on December 25, 2011, are shown as example in Figure 3, for the emissions at HXR and radio wavelengths. As seen in Figure 3, the high-energy x-ray data from RHESSI (50–300 keV) and the radio observations exhibit similar temporal evolution, with a few peaks. This correlation suggests that both emissions originate from the same population of accelerated electrons. These electrons likely emit gyrosynchrotron radiation as they spiral along magnetic loops and subsequently deposit their energy into the chromosphere upon encountering positive nuclei, leading to bremsstrahlung emission.

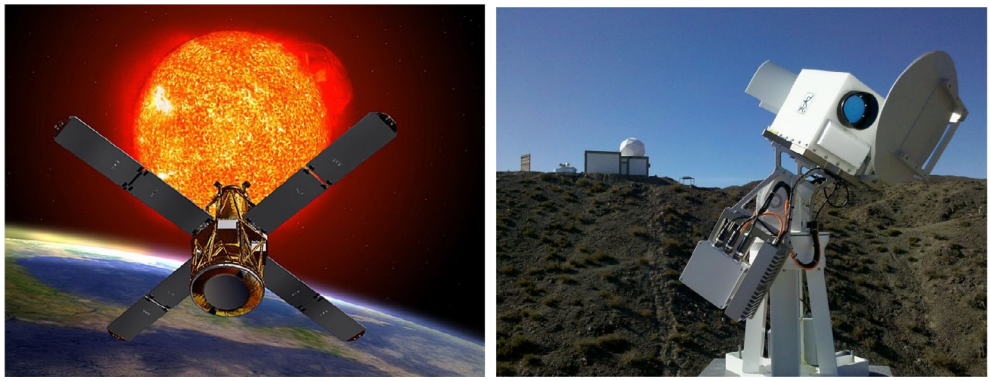

FIGURE 2 | Left: RHESSI space satellite (Lin et al. 2004). Right: The POEMAS telescope system at CASLEO, Argentina (Valio et al. 2013).

TABLE 1 | List of 10 selected events: Date, peak number, peak time, GOES spectral class, spectral indices of x-ray and microwave emission.

Date	Peak	Time (UT)	GOES class	δ_X	δ_r	Δ_{x-r}
December 25, 2011	1	18:15:01	M4.0	4.82	2.17	2.65
December 25, 2011	2	18:15:03		5.96	1.95	4.01
March 3, 2012	1	17:23:01	M7.9	4.21	2.25	1.96
March 13, 2012	2	17:23:05		4.50	2.20	2.30
June 3, 2012	1	17:53:19	M3.3	4.06	2.25	1.81
June 3, 2012	2	17:53:57		4.28	2.04	2.24
July 10, 2012	1	15:30:22	C2.2	4.73	3.80	0.93
July 10, 2012	2	15:30:50		4.76	3.76	1.00
November 27, 2012	1	15:56:02	M1.6	3.79	2.30	1.49
November 27, 2012	2	15:56:17		3.67	2.22	1.45
May 13, 2013	1	16:04:00	X2.8	4.10	2.10	2.00
October 26, 2013	1	19:24:59	M3.1	3.23	2.13	1.10
October 26, 2013	2	19:25:17		3.30	2.28	1.02
November 5, 2013	1	18:10:10	M1.0	4.83	2.85	1.98
November 6, 2013	1	13:43:09	M3.8	4.66	3.27	1.39
November 6, 2013	2	13:43:19		5.05	3.12	1.93
November 7, 2013	1	14:23:43	M2.4	5.59	2.96	2.63

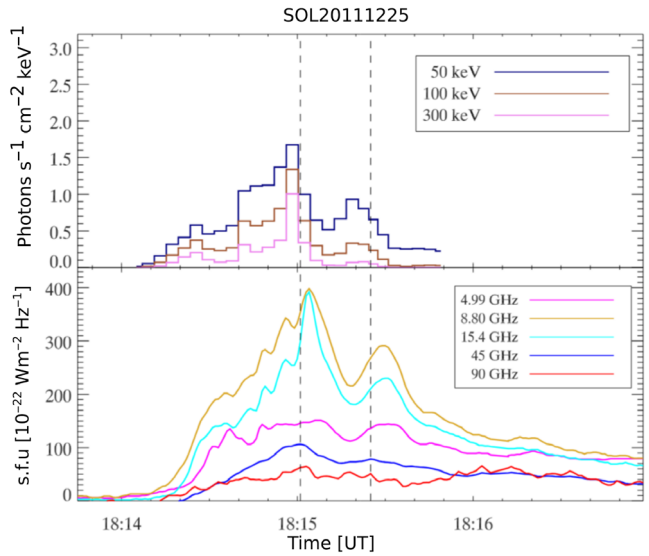

FIGURE 3 | Light curve of the December 25, 2011 flare at 50, 100, and 300 keV hard x-rays (top panel), and radio wavelengths, from 5 to 90 GHz (bottom panel).

Therefore, the HXR spectra and the radio spectra reveal insights into the physical processes governing particle acceleration and energy distribution during these events. From these spectra, two key indices can be measured: the x-ray photon spectral index, γ, and the optically thin radio spectral index, δ, both of which provide information about the nonthermal electron population generating the HXR and radio emissions. Comparing these indices help refine our understanding of flare energetics, allowing us to better characterize the mechanisms driving particle acceleration.

4 | Spectral Indices

The indices γ and δ were measured from the HXR and radio spectra in the way described in Section 2.1, where the accelerated electron spectral distribution indices were inferred from Equations (5) and (6), respectively. The indices of the events are listed at the fourth and fifth column of Table 1, as well as the difference $\Delta_{X-r} = \delta_X - \delta_r$. The flare on May 13, 2013 will be discussed separately in Section 4.1.

Histograms of the inferred spectral indices are shown in Figure 4. The data presented in Table 1 and Figure 4 clearly show that the inferred HXR spectral index, δ_X is always larger than δ_r from the radio observation. The average difference being $\Delta_{X-r} = 1.8 \pm 0.8$.

The observed x-rays below 100 keV are believed to emitted by electrons with energies up to 300 keV, while radio emissions are produced by electrons with much higher energies, typically above 1 MeV (White and Kundu 1992). This difference in energy ranges suggests a broken power-law distribution in the electron energy spectrum, where electrons of distinct energies contribute to the emissions observed in x-rays and radio frequencies. The break in the power-law reflects a possible different acceleration mechanisms associated with these energy ranges. This result was known previously from a similar comparison of HXR BATSE data and OVRO radio observations (Silva, Wang, and Gary 2000). Thus the scenario that emerges is that of a broken power-law at energy around 600 keV and a discrepancy in spectral index of $\delta_X - \delta_r \simeq 2$. Such a spectrum is exemplified in Figure 5, and is believed to be the case for the flares analyzed here rather than the spectrum shown in the top panel of Figure 1.

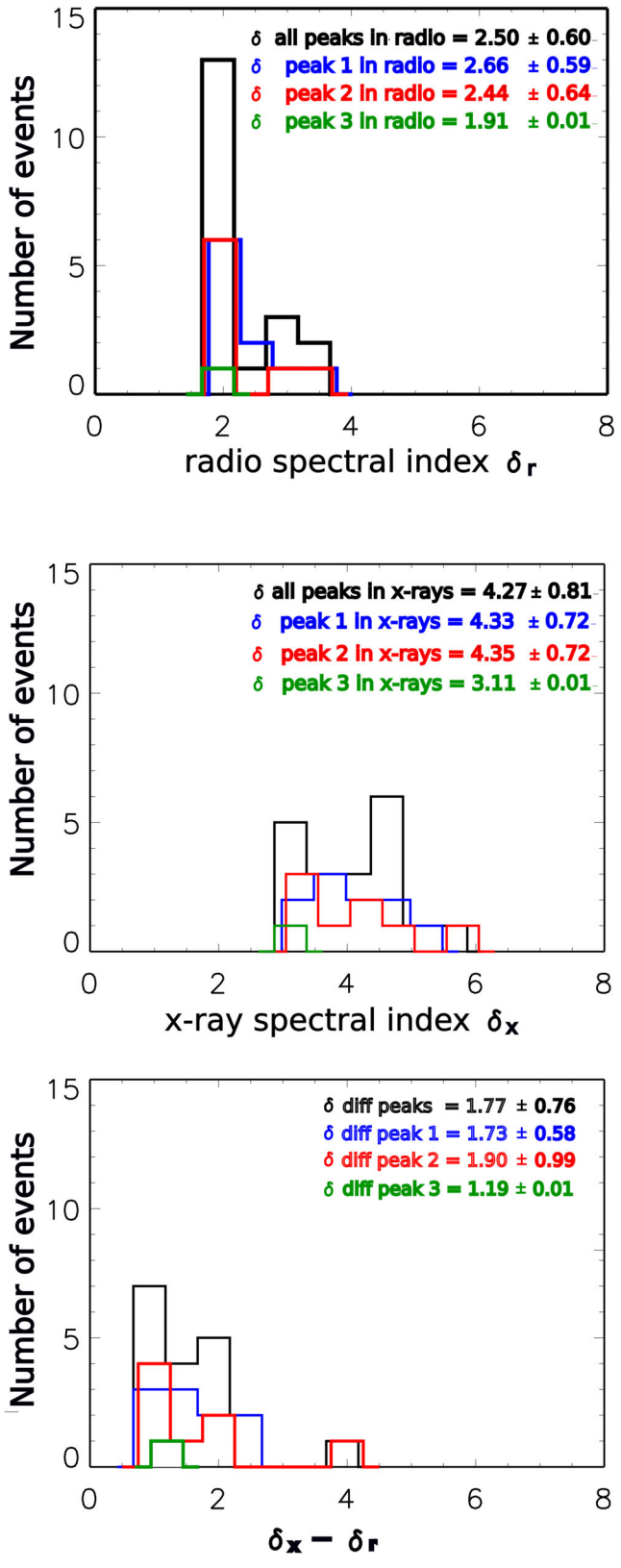

FIGURE 4 | To panel: Spectral index from radio spectra, δ_r. Middle panel: Spectral index from HXR observations, δ_X. Bottom panel: Difference between the spectral indices: $\delta_X - \delta_r$.

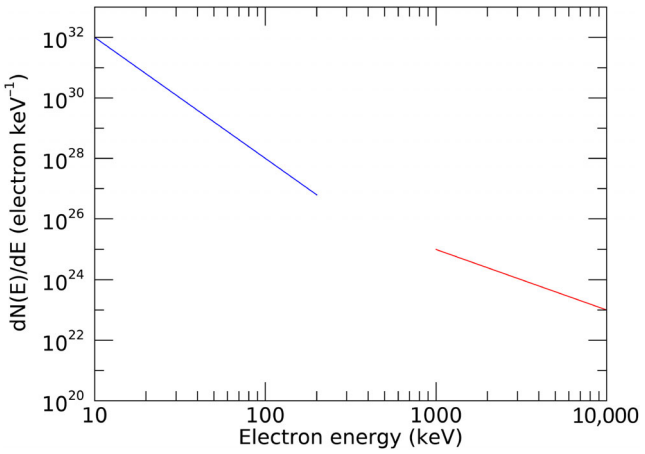

FIGURE 5 | Schematics of the broken power-law energy distribution of accelerated electrons. The HXR usually probe the blue part of the spectrum, whereas the radio emission originates from electrons with energies in the red part of the spectrum.

TABLE 2 | Results of the fit to the radio and hard x-ray spectra, for the three peaks in time of the flare.

	Interval 1	Interval 2	Interval 3
δ_r	2.1 ± 0.1	2.1 ± 0.1	2.1 ± 0.1
δ_X ($\leq E_2$)	4.1 ± 0.1	4.03 ± 0.03	3.99 ± 0.03
δ_X($\geq E_2$)	2.2 ± 0.4	2.9 ± 0.3	2.6 ± 0.6

4.1 | The Flare of May 13, 2013

The X2.8 solar flare on May 13, 2013, was observed at millimeter and centimeter wavelengths, as well as x-rays exceeding 1 MeV (da Silva and Valio 2021). The radio data were collected using the POEMAS telescope system, alongside microwave observations (1–15 GHz) from the RSTN. Concurrently, x-ray emissions for this event were recorded by the RHESSI and Fermi (Atwood et al. 2009) satellites.

Spectral data at both wavelengths were generated and fitted independently to determine the energy distribution of the accelerated electrons responsible for the emissions. The optically thin radio spectral index, δ_r given by Equation (6), was derived using the Ramaty model of gyrosynchrotron emission, while the (HXR) spectral index, δ_X given by Equation (5), was obtained by fitting a thermal emission model with a nonthermal broken power-law distribution (see Table 2). This broken power-law exhibited indices of ∼4 below a break energy $E_2 = 400-700$ keV and a harder index of 2–3 above these energies (da Silva and Valio 2021). Only electrons with energy above 100 keV were considered. This was the only flare among the ten events analyzed here in which photons exceeding 1 MeV were detected.

Comparing the two indices obtained for this event revealed that the radio spectral index, δ_r, aligns with the x-ray index, δ_X for

energies above approximately 600 keV. This finding supports the conclusion that (HXR) above 600 keV and high-frequency radio emissions in solar flares are produced by the same population of high-energy electrons. The results of the May 13, 2011 (da Silva and Valio 2021), suggest that these electrons follow an energy distribution characterized by a broken power–law, with a transition occurring at energies around 400–700 keV, like the one shown in Figure 5.

5 | Conclusions

Here we have performed an in-depth analysis of 10 solar flares, during the solar maximum period of 2012 and 2013, by examining their emissions in both radio and (HXR). The radio spectra of the flares were constructed from RSTN (2–15 GHz) and POEMAS (45 and 90 GHz) observations, whereas the (HXR) spectra were obtained from RHESSI and Fermi telescopes in the case of the May 13, 2013, event. The spectral parameters for each event were determined using gyrosynchrotron emission for radio wavelengths and a combined thermal and nonthermal model for (HXR).

The initial findings revealed a consistent discrepancy between the spectral indices of nonthermal electron populations in millimeter-wave and x-ray emissions, with the radio spectral index being notably harder by about 2 units. This result supports previous observations and suggests a break in the energy distribution of the accelerated electrons. This apparent discrepancy in spectral indices in the energy distribution of accelerated electrons in solar flares has been reported previously (Silva, Wang, and Gary 2000).

Notably, in the case of the flare on May 13, 2013, where photon energies exceeded 1 MeV, the indices matched for electrons with energies above ∼600 keV, indicating a shared electron population responsible for emissions in both HXR and radio. Below this energy, the spectral index δ_X is ∼4, while above it, δ_X reduces to about 2–3 (Table 2). This reinforces the presence of a broken power-law distribution in the electron energy spectrum and highlights the complex nature of particle acceleration in solar flares.

Millimeter-wave emissions, for instance, are produced by electrons with energies > 1 MeV (White and Kundu 1992), while x-ray emissions, especially those up to 200 keV observed in C and M-class flares, are generated by electrons with energies below 400 keV. Only when a large X flare is produced with energetic photons (≥ 1 MeV) do the indices match.

There are three potential explanations for this discrepancy between the indices:

1. The presence of two sources of energetic electrons, each generated by distinct acceleration mechanisms at a different location.
2. Diffusive shock acceleration (Li et al. 2013), which could cause spectral hardening around 500–600 keV. Alternatively, stochastic acceleration due to wave–particle interactions in the presence of Coulomb collisions (Hamilton and Petrosian 1992) may play a role.
3. The trap-plus-precipitation model (Lee and Gary 2000), in which lower-energy electrons escape from the trap due to Coulomb collisions, leaving the higher-energy electrons confined near the loop-top.

These explanations highlight the complexity of particle acceleration in flares and the need for further investigation into the physical processes involved. This scenario provides a coherent explanation for the observed x-ray and radio signatures, linking them to the dynamics of electron acceleration and energy transfer in solar magnetic fields.

Acknowledgments

A.V. acknowledges partial support from Brazilian agency FAPESP (grants #2018/04055-8 and #2021/02120-0). D.F.S. acknowledges the support from the China-Brazil Joint Laboratory for Space Weather (CBJLSW) for supporting his postdoctoral. This work was supported by the International Partnership Program of Chinese Academy of Sciences (Grants 183311KYSB20200003 and 183311KYSB20200017). H.L. acknowledges the support by NNSFC grants (42374198 and 42188101).

Conflicts of Interest

The authors declare no conflicts of interest.

References

Atwood, W. B., A. A. Abdo, M. Ackermann, et al. 2009. "The Large Area Telescope on the Fermi Gamma-Ray Space Telescope Mission." *Astrophysical Journal* 697, no. 2: 1071–1102.

da Silva, D. F., and A. Valio. 2021. "Broken Power-Law Energy Spectra of the Accelerated Electrons Detected in Radio and Hard X-Rays During the SOL2013-05-13 Event." *Astrophysical Journal* 915, no. 1: L1.

Dulk, G. A. 1985. "Radio Emission From the Sun and Stars." *Annual Review of Astronomy and Astrophysics* 23: 169–224.

Guidice, D. A., E. W. Cliver, W. R. Barron, and S. Kahler. 1981. "The Air Force RSTN System. In." *Bulletin of the American Astronomical Society* 13: 553.

Hamilton, R. J., and V. Petrosian. 1992. "Stochastic Acceleration of Electrons. I. Effects of Collisions in Solar Flares." *Astrophysical Journal* 398: 350.

Lee, J., and D. E. Gary. 2000. "Solar Microwave Bursts and Injection Pitch-Angle Distribution of Flare Electrons." *Astrophysical Journal* 543, no. 1: 457–471.

Li, G., X. Kong, G. Zank, and Y. Chen. 2013. "On the Spectral Hardening at gsim300 keV in Solar Flares." *Astrophysical Journal* 769, no. 1: 22.

Lin, R. P., B. Dennis, G. Hurford, D. M. Smith, and A. Zehnder. 2004. "The Reuven Ramaty High-Energy Solar Spectroscopic Imager (RHESSI) Mission." In *Telescopes and Instrumentation for Solar Astrophysics, Volume 5171 of Society of Photo-Optical Instrumentation Engineers (SPIE) Conference Series*, edited by S. Fineschi and M. A. Gummin, 38–52. (San Diego, CA: Society of Photo-Optical Instrumentation Engineers (SPIE)).

Lin, R. P., and Rhessi Team. 2002. "RHESSI Observations of Particle Acceleration in Solar Flares." In *Solar Variability: From Core to Outer Frontiers*, edited by A. Wilson, vol. 2, 1035–1044. (Noordwijk: of ESA Special Publication).

Shibata, K., and T. Magara. 2011. "Solar Flares: Magnetohydrodynamic Processes." *Living Reviews in Solar Physics* 8, no. 1: 6.

Silva, A. V. R., H. Wang, and D. E. Gary. 2000. "Correlation of Microwave and Hard X-Ray Spectral Parameters." *Astrophysical Journal* 545, no. 2: 1116–1123.

Tandberg-Hanssen, E., and A. G. Emslie. 2009. *The Physics of Solar Flares*. (Cambridge, UK: Cambridge University Press).

Valio, A., P. Kaufmann, C. G. Giménez de Castro, J.-P. Raulin, L. O. T. Fernandes, and A. Marun. 2013. "Polarization Emission of Millimeter Activity at the Sun (POEMAS): New Circular Polarization Solar Telescopes at Two Millimeter Wavelength Ranges." *Solar Physics* 283: 651–665.

White, S. M., and M. R. Kundu. 1992. "Solar Observations With a Millimeter Wavelength Array." *Solar Physics* 141, no. 2: 347–369.